Intrinsic localized spin waves in classical one-dimensional spin systems: Studies of their interactions

S. Rakhmanova and D. L. Mills
Department of Physics and Astronomy, University of California, Irvine, California 92697
(Received 24 March 1998; revised manuscript received 6 July 1998)

One-dimensional classical spin systems can support nonlinear excitations referred to as intrinsic localized spin-wave modes. These entities have internal frequencies which lie outside the spin-wave bands of linear theory, and are localized by virtue of the intrinsic nonlinearity present in spin systems. By numerical methods, we have explored collisions between these objects. We explore the influence of a defect on the spectrum of intrinsic nonlinear spin waves, to find a new class of modes localized at the defect. We also examine the interaction of a propagating nonlinear mode with the defect, to find rich behavior. The mode may be transmitted with no reflected component, trapped or reflected depending on the strength of the perturbation associated with the defect spin. [S0163-1829(98)01841-4]

I. INTRODUCTION

For many decades, since the work of Bloch in the early 1930s,[1] it has been known that in Heisenberg magnets, the elementary excitations are spin waves. These extended, plane-wave modes control the thermodynamics of such systems at low temperatures. In the late 1970s and early 1980s,[2] attention was directed toward unique aspects of one-dimensional Heisenberg magnets. If the spins are viewed as classical objects and suitable anisotropy is present, the equations of motion admit static domain-wall solutions, and solutions in which such walls move with finite velocity. That this is so quite generally had been known much earlier.[3] The unique aspect of the one-dimensional spin chain is that the excitation energy is on the microscopic scale. Thus, moving domain walls may be excited thermally, and contribute to the thermodynamics of the system. At low temperatures, the thermal excitations may be viewed as a dilute soliton gas, with spin waves present as well.

In the recent literature, considerable theoretical attention has been devoted to objects referred to as intrinsic localized spin modes (ILSM states).[4–6] These are localized entities, stabilized by the intrinsic anharmonicity inherent in the equations of motion of the spin system; so far primary attention has been directed toward the one-dimensional line of classical spins. These entities differ in one important, qualitative regard, when compared to the domain-wall structures discussed some years ago.[2] When the ILSM is at rest, all spins in the system are engaged in circular precession, at some frequency Ω which lies outside the frequency bands associated with the spin waves of linear theory. In contrast to this, when the domain walls described in the previous paragraph are at rest, the spins are static. The ILSM states are found to exist for *any* internal frequency Ω above the linear spin-wave bands, in a model we have studied. For a one-dimensional line of a finite number N of spins, we have demonstrated previously that for any such frequency Ω, the equations of motion also admit solutions with two, three, four,... intrinsic localized spin-wave modes.[5]

The studies that have appeared to date have explored the properties and nature of these states for various models and circumstances. A complete review of localized spin excitations and their properties is provided by Kosevich, Ivanov, and Kovalev,[7] though the ILSM's just described are not discussed. In the present paper, we address interactions experienced by intrinsic nonlinear spin-wave modes. We first examine collisions between two such modes. The behavior we find here is complex. There are circumstances where the modes emerge from a collision unchanged in shape or form, and thus behave as solitons. However, more generally, we see spin waves emitted as a consequence of such a collision, so, in fact, these localized entities interact in a complex manner. We provide several examples. In what follows, we use the term soliton to describe these modes on occasion, but the reader should appreciate their interactions are complex.

We also place a defect in our one-dimensional line of spins and find a class of ILSM's localized on the defect. We then study the interaction of the ILSM solitons with the defect spin, to find very rich behavior. If the perturbation presented by the defect is weak, the soliton passes over it with a transmissivity of unity, though its center-of-mass velocity is altered. Upon increasing the strength of the perturbation, we reach a regime where the entity is self-trapped. Then a further increase in strength of the perturbation takes us into a domain where the soliton is reflected completely. In this latter regime, the soliton may be trapped between two defects.

One may inquire if one may realize a physical system described by a model Hamiltonian such as that employed here and in our earlier studies. Magnetic superlattices can be synthesized which meet this requirement. An ultrathin magnetic film in such a structure is characterized by its total magnetization $\mathbf{M}(t)$, which may be viewed as a classical spin. Two neighboring such ''spins'' can experience ferromagnetic couplings such as contained in our model, by fabricating a structure with appropriate nonmagnetic films sandwiched between the ferromagnetic films. It is possible to synthesize easy-plane ferromagnetic films, with very small in-plane anisotropy. Thus, the ground state is ferromagnetic, with spins in the plane normal to the growth axis of the superlattice. We consider such a system, with spins pulled into ferromagnetic alignment by a magnetic field perpendicular to the easy plane. Note that for a superlattice in this configuration, when the moments precess, no intrafilm de-

magnetizing fields are generated by the spin motion. Thus, such a superlattice is a physical realization of the model system studied here. Other authors have demonstrated that ILSM's exist for other model one-dimensional spin systems.[6,8]

This paper is organized as follows. In Sec. II, we present the model and discuss issues related to solving the equations of motion for moving ILSM solitons. Section III presents our studies of collisions between moving solitons. Section IV examines the nonlinear modes localized on a defect, and Sec. V the interaction of ILSM solitons with magnetic defects.

II. INITIAL CONDITIONS AND PROPAGATION OF A SINGLE LOCALIZED MODE THROUGH A PERFECT CHAIN

We consider a ferromagnetic chain of N spins described by the Hamiltonian

$$\hat{\mathbf{H}}=-2J\sum_n \mathbf{S}_n\cdot\mathbf{S}_{n+1}+A\sum_n (S_n^z)^2-H_0\sum_n S_n^z, \qquad (1)$$

where $J>0$ is the exchange interaction constant, A is the anisotropy constant, and H_0 is the magnitude of the external field applied along $\hat{z}$ axis. We chose A positive, which corresponds to the case of easy-plane anisotropy. The field H_0 is assumed to be large enough so that in the ground state all spins are ferromagnetically ordered along the $\hat{z}$ axis. The equation of motion for the nth spin is found from

$$i\hbar\,\frac{d\mathbf{S}_n}{dt}=[\mathbf{S}_n,\hat{\mathbf{H}}]. \qquad (2)$$

After obtaining the commutator of the spin operator with the Hamiltonian in Eq. (2), we treat operators $\mathbf{S}_n$ as classical vectors of magnitude S. To bring the equations of motion into suitable form, we introduce vectors s_n^+ and s_n^z defined by $s_n^+=(S_n^x+iS_n^y)/S$, $s_n^z=S_n^z/S$. We separate fast scale oscillations by writing s_n^+ in the form $s_n^+=[s_n^x(t)+is_n^y(t)]e^{i(kn-\omega t)}$. Then, the complex amplitude $s_n(t)=s_n^x(t)+is_n^y(t)$ obeys

$$\frac{ds_n}{d\tau}=i[\Omega s_n-s_n(\sqrt{1-|s_{n+1}|^2}+\sqrt{1-|s_{n-1}|^2})+(2Bs_n+(s_{n+1}+s_{n-1})\cos k)\sqrt{1-|s_n|^2}]-(s_{n+1}-s_{n-1})\sin k\sqrt{1-|s_n|^2} \qquad (3)$$

with $\Omega=(\omega-H_0)/2JS$, $B=A/J$, and $\tau=(2JS/\hbar)t$. Here, s_n^z is replaced by $\sqrt{1-|s_n|^2}$, since the magnitude of $\mathbf{s}_n$ is conserved, and explicit dependence of s_n's on time is dropped for the sake of brevity. We use free end boundary conditions. Therefore, the evolution of the end spins $n=1$ and $n=N$ is described by Eq. (3) without the term s_{n-1} for $n=1$ and the term s_{n+1} for $n=N$. Equation (3) together with the boundary conditions constitute the basis of our numerical calculations. Supplemented by proper initial conditions, it is solved on a computer by fourth-order Runge-Kutta method.

To integrate Eq. (3) forward in time, we need an initial set of values for $s_n(0)$. So far as we can see, if we assume that a stable, moving ILSM exists for a given choice of Ω and k, there is no way of determining its form in advance of actually solving the equations of motion. There is no analytical solution to use as a guide, in general. When Ω is very close to the top of the linear spin-wave bands, we may introduce a continuum approximation, and one is led to the nonlinear Schrödinger equation.[4] We have proceeded here with the following viewpoint. If we choose a set of $s_n(0)$ which describes a form close to but not a perfect representation of a stable ILSM, then at short times this object will shed energy in the form of spin waves, and settle down into a stable object, moving with some velocity v. The spin waves give rise to a slightly noisy background. We have found that the following procedure works well over a wide parameter domain. By this last statement, we mean the background noise has very small amplitude, after the solution settles down.

The initial conditions are chosen so that the Eq. (3) will describe the propagation of the ILSM through the finite chain of spins, as just discussed. It is also desirable that for the case $k=0$, these initial conditions generate the stationary ILSM familiar from Ref. 5. The best way to proceed, in our experience, is to generalize to nonzero k the equation the stationary ILSM's satisfy. Here we make use of the following observation. Let us assume for the moment that at $\tau=0$ the quantity in square brackets on the right-hand side of Eq. (3) vanishes. Thus, the initial configuration satisfies

$$\Omega s_n(0)=s_n(0)[\sqrt{1-|s_{n+1}(0)|^2}+\sqrt{1-|s_{n-1}(0)|^2}]-\{2Bs_n(0)+[s_{n+1}(0)+s_{n-1}(0)]\cos k\}\sqrt{1-|s_n(0)|^2}. \qquad (4)$$

Then, given $s_n(0)$ from Eq. (4), we find that the equation $ds_n/d\tau=-\sin k(s_{n+1}-s_{n-1})\sqrt{1-|s_n|^2}$ determines the evolution of the system at least during the first few time steps. For small s_n it describes uniform propagation of the initial profile as a whole without changing its shape. The velocity of propagation is equal to $-2\sin k$, as one can see if one writes the equation in the form $ds_n/d\tau+2\sin k(s_{n+1}-s_{n-1})/2\approx 0$.

In numerical calculations we proceed as follows. We find a solution of stationary Eq. (4) and use it as an initial configuration for the full time-dependent Eq. (3). Note that s_n is complex in both equations. The linear spin-wave bands associated with Eq. (4) lie in the frequency region Ω from $-2B$ to $4-2B$. For all calculations discussed here we use the anisotropy constant $B=4$, the same value as in Ref. 5. Then, the linear spectrum corresponds to $-8<\Omega<-4$. We find that for any value of k Eq. (4) also has localized solutions, with frequencies above the linear spin-wave band. The amplitude and degree of localization of these solutions are now determined not only by Ω, B, but also by k. When k equals zero they are the stationary ILSM's of Ref. 5. If Ω is close to the linear spin-wave band region, and k is not too large, then the amplitude of the ILSM is small and it propagates without loss of its shape. We first consider a solution of Eq. (4) for $N=501$ in the form of a single localized excitation with $\Omega=-3.85$ and $k=0.1$. The evolution of this excitation is illustrated in Fig. 1 where we plot $|s_n(\tau)|^2$ at each site. The ILSM travels through the chain with a constant speed and reflects elastically from the boundaries. The velocity of the propagation is very close to the estimated value

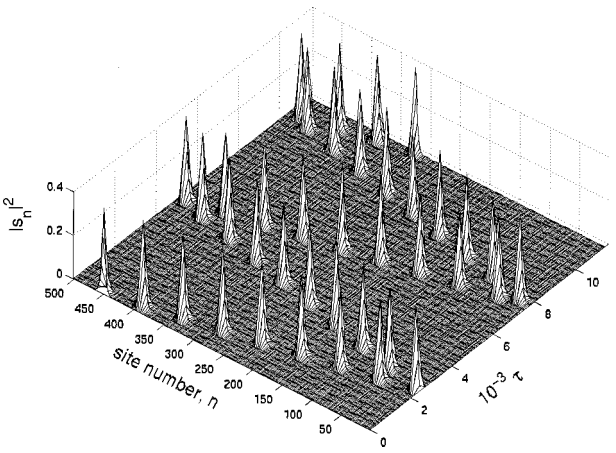

FIG. 1. The time evolution, as determined by Eq. (3), of the initial configuration taken as the solution of Eq. (4) in the form of a single soliton with $\Omega=-3.85$ and $k=0.1$. The chain consists of 501 identical spins.

$-2\sin k$. The excitation remains stable and shows little signs of decay even after a very long run.

This method of initialization of the traveling ILSM's works quite well for frequencies Ω close to the top of the linear spin-wave band and small wave numbers k. For larger Ω's but k still small we observe a slowdown, stopping, and finally reversal of direction of the propagation of the ILSM, which is in agreement with the results of Ref. 7 for antiferromagnetic chains. If both Ω and k are large in the Eq. (4), then during the evolution the starting configuration experiences relaxation into an ILSM with lower amplitude before it begins to move. This process is accompanied by energy release in the form of low amplitude extended spin waves. The remaining localized entity moves freely through the chain as pictured in Fig. 2. Clearly, while we have achieved a stable ILSM, our initial guess is sufficiently far removed from the final stable profile that a substantial fraction of the initial energy is shed by the structure. Note the ''Cerenkov wake.'' A spectral analysis of this ILSM shows that its frequency Ω has changed and is smaller than the value that was used in Eq. (4) for obtaining the initial envelope.

The procedure outlined above differs considerably from that used in Ref. 7. Once we chose the initial values $s_n(0)$ by

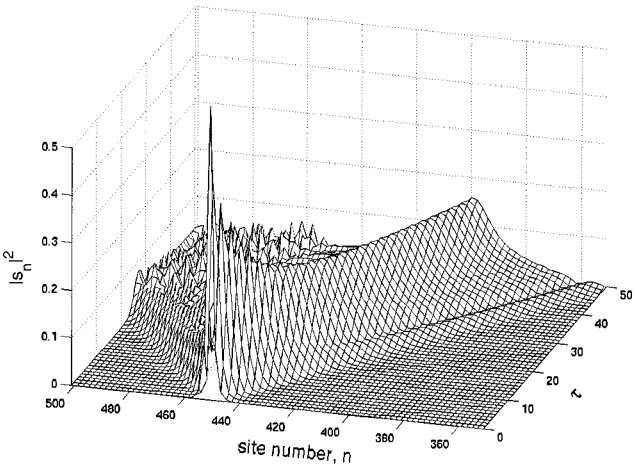

FIG. 2. The same as in Fig. 1, but the value of the wave number k is much larger, $k=0.9$.

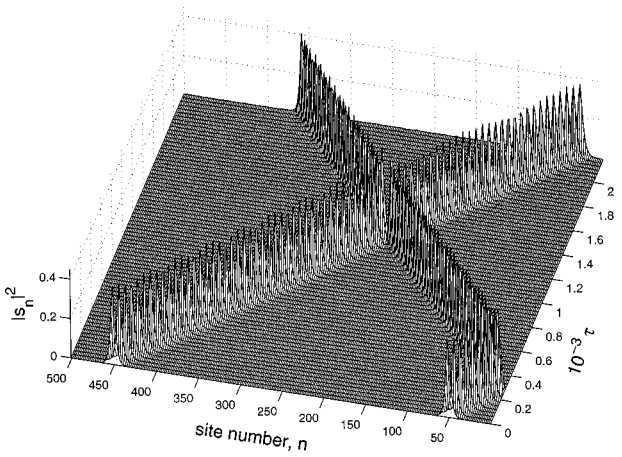

FIG. 3. Collision of two ILSM solitons. Each has $\Omega=-3.85$ and $k=0.1$, due to the fact that they were obtained by taking as the initial configuration a two-soliton solution of Eq. (4).

the method just outlined, at all future times we are solving the *full* equation of motion, Eq. (3), for each spin in our system. The authors of Ref. 7 assume $s_n(\tau)$ to be real at all times. They choose $s_n(0)$ by requiring the quantities inside the square brackets of Eq. (3) to vanish. They then project forward in time by requiring

$$\frac{ds_n}{d\tau}=-(s_{n+1}-s_{n-1})\sin k\sqrt{1-|s_n|^2} \tag{5}$$

for all times. Note this procedure assumes the quantity in square brackets in Eq. (3) vanishes at *all* times, and not just $\tau=0$. We have checked explicitly whether this assumption is valid by using their method to find $s_n(0)$, but then solving the full Eq. (3) for all times. We find the terms in square brackets to vanish only at short times; one is required to solve the full time-dependent equation, unfortunately, once the initial configuration is chosen.

III. COLLISIONS BETWEEN TWO ILSM'S ON THE PERFECT CHAIN

In this section, we present studies of collisions between two ILSM's. In Fig. 3 we show an example of such a collision. To generate this figure, we have proceeded as follows. We have a line of 501 spins. We then, for $k=0.1$ and the frequency $\Omega=-3.85$ (recall the top of the linear spin-wave band is at $\Omega=-4.0$), find at $\tau=0$ a two-soliton solution of Eq. (4); as we have demonstrated earlier,[5] for the finite line, multisoliton solutions exist. As we start the integration of Eq. (3) in time, both ILSM's in the solution move to the right at the same speed. The rightmost feature reflects off the right end of the line, and subsequently the two approach each other and collide. It is evident from the figure that they remain unchanged in shape.

If we regard the two solitons in Fig. 3 as independent entities, then each has precisely the same internal frequency Ω, and wave vector k. One may inquire if this is perhaps a special case. This does not appear to be so, as we illustrate in Fig. 4.

At time $\tau=0$, we create two distinct objects as follows. We find a single soliton solution on the line of 501 spins for

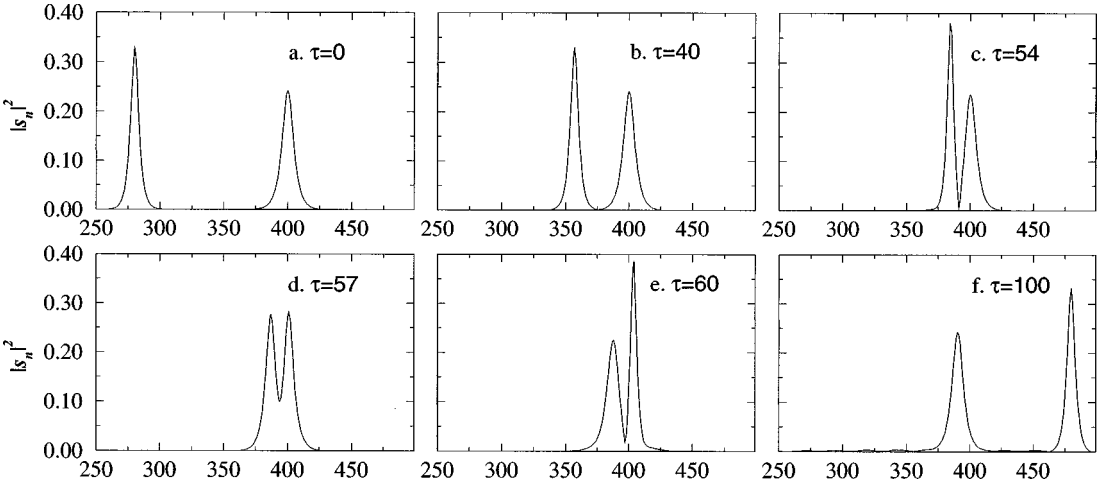

FIG. 4. Collision of two ILSM solitons, one has $\Omega=-3.90$ and $k=0.1$, and another has $\Omega=-3.95$ and $k=0$. The ILSM solitons are initiated as two different single-soliton state solutions of Eq. (4) with corresponding parameters Ω and k.

$\Omega=-3.90$ and $k=0.1$, and then we find a second single soliton state for $\Omega=-3.95$ and $k=0$ on the same line. We set up $s_n(0)$ by placing the $\Omega=-3.90$ mode on the left side of the line, and the $\Omega=-3.95$ mode on the right side of the line. The initial configuration is illustrated in Fig. 4(a). Then we integrate the *full* equations of motion, Eq. (2) forward in time; we cannot use Eq. (3) because, of course, it assumes we have a single frequency Ω and wave vector k everywhere on the line. When we carry out this calculation, we use the three equations of motion, for s_n^x, s_n^y, and s_n^z, respectively.

We see in Fig. 4(b) that the leftmost soliton moves to the right, and approaches the rightmost one, which remains stationary. We see the two collide, and Fig. 4(f) shows that in the final state, each emerges unchanged in shape. Note that there is one small effect of the interaction. The $k=0$ mode has been displaced very slightly to the left, after the collision has been completed.

If one looks closely at Fig. 4(f), one sees very small-amplitude spin waves that have appeared. In our view, to the level of accuracy of our simulation, it is not clear that these features are significant. Keep in mind our discussion of Sec. II, where the precise procedure for setting up the spins at $\tau=0$ is not clearly defined. Such very small-amplitude spin waves may well be a reflection of the fact that at $\tau=0$, the stable ILSM has not quite been depicted accurately.

In Fig. 4, each ILSM has an internal frequency very close to the top of the linear spin-wave bands. As a consequence of this, the envelopes of each extends over quite a few lattice constants. As noted earlier, in this limit, one may use the continuum approximation, and Eq. (3) may be mapped into the nonlinear Schrödinger equation.[4] In fact, the envelope function of each ILSM is reproduced nicely by this continuum approximation. Since the nonlinear Schrödinger equation is well known to admit multisoliton solutions, and these entities are noninteractive, one may suppose the result in Fig. 4 is, thus, expected. However, the internal frequency of each ILSM in such a multisoliton solution is identical, while we have two distinctly different internal frequencies for the objects in Fig. 4.

At this point, one is tempted to conclude that the ILSM's have solitonic properties. Further studies show this is not the case. We return to the case examined in Fig. 3, where the internal frequency $\Omega=-3.85$. We noted earlier,[5] that there are two distinct solutions of Eq. (3) for a given choice of Ω. This is because the equation of motion is invariant under $s_n\rightarrow -s_n$. The second differs from the first by a 180° phase shift. We thus have two ILSM's which, in some sense, may be regarded as degenerate. (In Ref. 5, the states were studied in the presence of an external, circularly polarized oscillating magnetic field in the *xy* plane. Such a field ''splits'' these two states, in a sense discussed in Ref. 5.) The collision illustrated in Fig. 3 is between two identical ILSM's. In Fig. 5, we show a collision between an ILSM with $\Omega=-3.85$ and a second such object with same internal frequency, but phase shifted by 180°. We now see a complex interaction between these two objects. In Fig. 6, we show another example. This is the interaction between an ILSM with an internal frequency of $\Omega=-3.90$, with a very localized ILSM at rest with $\Omega=-2.00$. Here the ILSM at rest acts like a perfectly reflecting barrier.

Interactions between ILSM's are, thus, complex in nature. We do realize, under the circumstances outlined, that these objects can behave in a manner similar to solitons, i.e., they pass through each other as if they are noninteracting par-

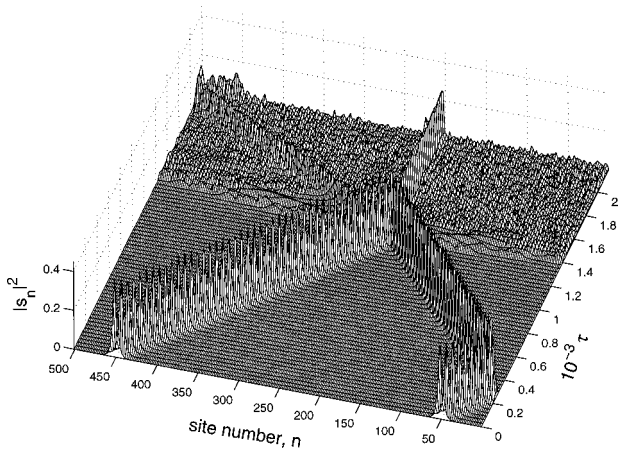

FIG. 5. Collision between two ILSM's. Each has $\Omega=-3.85$ and $k=0.1$. The initial configuration is same as for Fig. 3, except that one of the ILSM's is phase shifted by 180° with respect to the other.

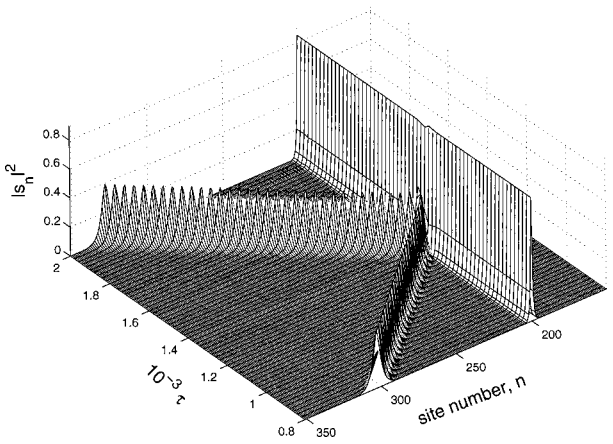

FIG. 6. Collision of a moving ILSM with low frequency ($\Omega = -3.90$) with stationary ILSM with high frequency ($\Omega = -1.00$).

ticles. But this behavior is not universal; the interactions may be complex in character.

IV. NONLINEAR SPIN-WAVE MODES LOCALIZED AT DEFECTS

So far we have explored the properties of ILSM solitons on the perfect lattice. Now we place a defect spin right in the middle of the line. We model the defect as follows. All spins on the line continue to interact with the same nearest-neighbor exchange interaction J. For the defect spin, we change the anisotropy constant from B, to $B-\Delta B$. A real defect in one-dimensional spin system will have exchange coupling to neighbors of magnitude different than found in the host, and the spin s may have different magnitude as well. While such effects are easily included in our model, without an explicit example in mind, a meaningful choice of such parameters is problematical. We wish to study the nonlinear properties of a system which, in linear theory, admits a localized spin mode above the spin-wave bands in frequency. We achieve this by simply decreasing the anisotropy constant of a selected spin, designated as the impurity. The resulting model then has just one parameter.

In the theory of the linearized excitations, when $\Delta B > 0$,

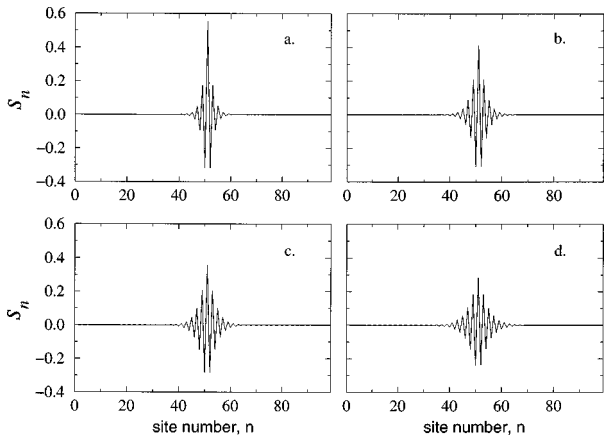

FIG. 7. Nonlinear modes localized at a defect for which $\Delta B/B = 0.03$. We show modes for the following frequencies: (a) $\Omega = -3.60$, (b) $\Omega = -3.80$, (c) $\Omega = -3.85$, and (d) $\Omega = -3.90$.

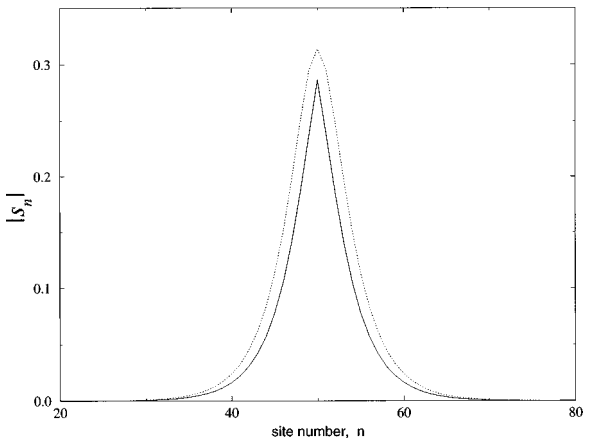

FIG. 8. Envelope functions of stationary ILSM on a perfect spin chain (showed by dotted line), and nonlinear localized mode trapped on a defect with $\Delta B/B = 0.03$. The internal frequency of both modes is $\Omega = -3.90$.

we always have a localized spin-wave mode pushed out of the top of the spin-wave bands of the linear theory. The local spin-wave mode thus resides in the frequency region where the ILSM's are found, for this sign of ΔB. For $\Delta B < 0$, a local mode emerges from the bottom of the spin-wave bands. When $\Delta B > 0$, if Ω_M is the maximum linear spin-wave frequency, that $\Omega_{\rm loc}$ of the local mode may be written

$$\Omega_{\rm loc} = \Omega_M + \Delta\Omega, \tag{6a}$$

where for our model

$$\Delta\Omega = 2\sqrt{1+(\Delta B)^2} - 2. \tag{6b}$$

We find that we have stationary, nonlinear localized mode solutions where the localized nonlinear mode is localized on the defect. These states can occur when the internal frequency Ω of the localized mode exceeds $\Omega_{\rm loc}$, the frequency for localized spin-wave modes in linear theory. For $\Delta B/B = 0.03$ we show the spatial form of the nonlinear localized modes in Fig. 7, for several frequencies. These modes have a spatial profile quite similar to the ILSM's on the perfect line, but have smaller amplitudes, as we see from Fig. 8, where

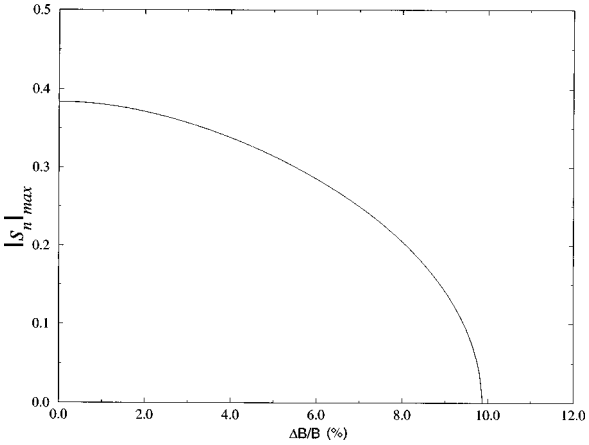

FIG. 9. Dependence of the amplitude of nonlinear mode localized at a defect site on the value of the defect perturbation. The frequency of the mode is $\Omega = -3.85$.

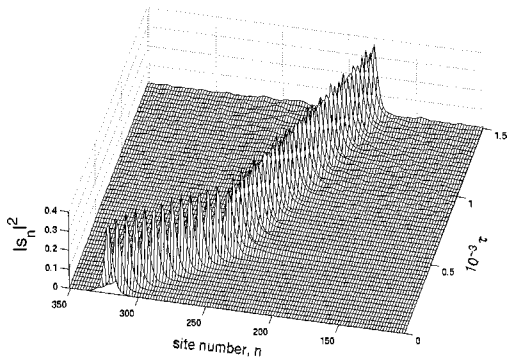

FIG. 10. Propagation of an ILSM soliton with $\Omega=-3.85$ through the spin chain with a defect. The defect spin is at site 251, and has the value $\Delta B/B=0.01$.

we make a comparison between the two. The amplitude of the nonlinear mode localized at a defect depends on the value of the perturbation associated with the defect. We illustrate this dependence in Fig. 9.

In Fig. 9, we show the following. For small $\Delta B/B$, we set up a localized ILSM, trapped on the defect. Then we examine the amplitude on the impurity of the ILSM, as $\Delta B/B$ is increased in magnitude with the internal frequency of the localized ILSM held fixed. We have $\Delta B/B$ positive always, so we have a defect which supports a localized spin-wave mode in linear theory. We see that as $\Delta B/B$ increases in magnitude, the amplitude of the localized ILSM decreases, to vanish when $\Omega_{\rm loc}$ equals its internal frequency Ω. We find no localized, nonlinear modes when $\Omega<\Omega_{\rm loc}$. We now turn to our studies of the interactions of propagating ILSM's with the defect.

V. INTERACTION OF PROPAGATING ILSM MODES WITH THE DEFECT

In the previous section, we saw that in the presence of a defect in the spin chain, we may have localized ILSM excitations, trapped on the defect. In this section, we study the interaction of moving ILSM's with the same defect. We illustrate the various characteristic regions through a sequence of figures. In all figures, the frequency of the propagating ILSM is set at $\Omega=-3.85$, and its wave vector $k=0.1$. We will vary the ratio $\Delta B/B$, as we study the interactions. We

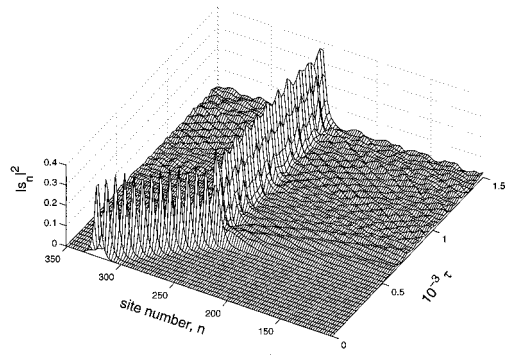

FIG. 11. Propagation of an ILSM soliton with $\Omega=-3.85$ through the spin chain with a defect. The defect spin is at site 251, and has the value $\Delta B/B=0.015$.

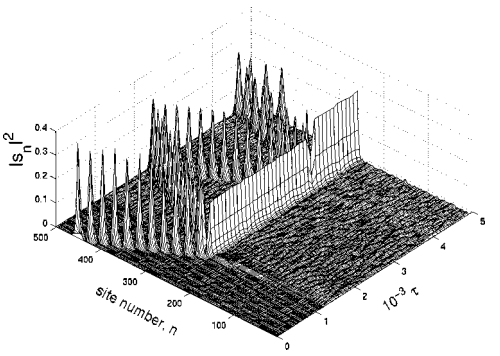

FIG. 12. Propagation of an ILSM soliton with $\Omega=-3.85$ through the spin chain with a defect. The defect spin is at site 251, and has the value $\Delta B/B=0.07$.

again have a line of 501 spins, with the defect at site 251.

In Fig. 10, we show the ILSM soliton passing by a defect characterized by a very small value of $\Delta B/B$, $\Delta B/B=0.01$. The soliton passes over the defect, with no reflected pulse. Clearly, its center-of-mass velocity has decreased rather appreciably. If one looks carefully at the figure, one sees no evidence of spin waves shed by the ILSM before collision. Afterward, however, one sees distinct small-amplitude excitations spread over the chain, outside the region of the ILSM soliton. So far as we can see, we have no excitation at the site of the defect, after the ILSM soliton has passed by. Evidently the slowdown has its origin in the energy shed in the form of spin waves. For $\Delta B/B=0.0075$, the slowdown is less pronounced, and the amplitude of the spin waves excited after the collision is much smaller.

As $\Delta B/B$ increases further, we enter a regime where the ''radiative loss'' of energy by the ILSM soliton is sufficient for this entity to become trapped on the defect. We illustrate this in Fig. 11 where we have $\Delta B/B=0.015$. So far as we can tell from the simulations, the trapped entity (presumably a localized ILSM such as that discussed in previous section) has an infinite lifetime. Clearly, it is perturbed periodically by interaction with the ''spin-wave radiation'' reflected from the ends of the chain. As $\Delta B/B$ increases yet further, however not exceeding the limit where $\Omega_{\rm loc}$ exceeds Ω, we see the build up of a reflected ILSM. In Fig. 12, where $\Delta B/B$

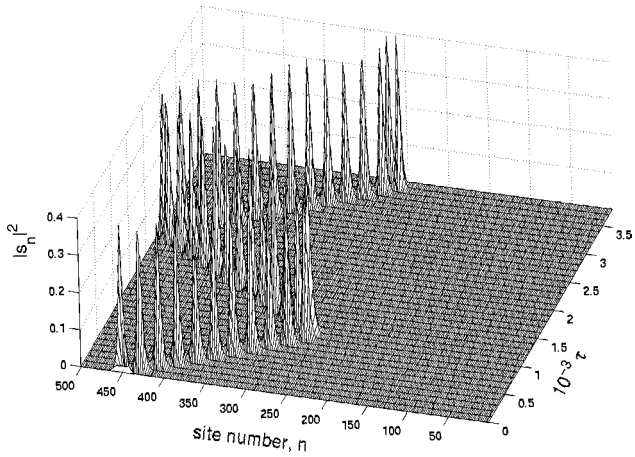

FIG. 13. Propagation of an ILSM soliton with $\Omega=-3.85$ through the spin chain with a defect. The defect spin is at site 251, and has the value $\Delta B/B=0.35$.

$=0.07$, we see well-defined reflected ILSM solitons, with energy stored continuously near the defect site, in the form of a localized ILSM soliton. Notice that the propagating soliton is trapped between the defect, and the end of the chain. Clearly, one could trap such a mode between two defects.

As we saw in the previous section, when the internal frequency is fixed, and $\Omega_{\rm loc}$ exceeds Ω, the defect fails to support a nonlinear ILSM. In this regime, the ILSM soliton is reflected off the defect; the reflection appears elastic, in the sense that in the simulations we see no evidence for radiated spin waves. We illustrate this in Fig. 13.

If $\Delta B/B<0$ in our model, in linear spin-wave theory, there is no spin-wave mode localized at the defect in the frequency region above the spin-wave bands. We find no localized nonlinear ILSM's as well. We find for $\Delta B/B<0$, the propagating ILSM is fully reflected from the defect, even when $\Delta B/B$ is as small as -0.0075. The interaction has an appearance very similar to Fig. 13. In this section, we have explored the interaction of ILSM solitons with defects, to find the rich behavior outlined above.

VI. CONCLUDING REMARKS

We have presented a method for simulating a moving ILSM numerically, starting from a stationary ILSM as the initial condition. We conclude that in the collisions with each other, ILSM's can exhibit solitonic properties, as illustrated by the examples provided. That is, they preserve their shape, speed, and identity after the collision. Generally, however, the interactions can be complex. It is possible to have stationary nonlinear localized excitation centered at the defect site. The internal frequency of this excitation has to be greater than the frequency of corresponding linear localized mode. The interaction of a moving ILSM with defects has diverse and rich character, depending on the relation of the internal frequency of the ILSM to the local mode frequency of linear spin-wave theory. If $\Omega_{\rm loc}>\Omega$, so that stationary nonlinear localization is not allowed on the defect, the traveling ILSM reflects elastically from the defect spin. In the range of the defect perturbations, for which nonlinear localization is possible, we observe a strong interaction between a traveling ILSM and a stationary nonlinear mode localized on the defect.

ACKNOWLEDGMENT

This research was completed with support from the Army Research Office, under Contract No. CS0001028.

[1] F. Bloch, Z. Phys. **61**, 206 (1930).

[2] H. J. Mikeska, J. Phys. C **11**, L29 (1978); **13**, 2913 (1980); see, also K. M. Leung, D. W. Hone, D. L. Mills, P. Riseborough, and S. E. Trullinger, Phys. Rev. B **21**, 4017 (1980). A discussion of moving solitons, with attention to circumstances where the simple relativistic analogy fails is given by P. S. Riseborough, S. E. Trullinger, and D. L. Mills, J. Phys. C **14**, 1109 (1981).

[3] A. P. Malozemoff and J. Sloncewski, *Magnetic Domain Walls in Bubble Materials* (Academic, New York, 1979).

[4] R. F. Wallis, D. L. Mills, and A. D. Boardman, Phys. Rev. B **52**, R3828 (1995); S. V. Rakhmanova and A. V. Shchegrov, *ibid.* **57**, R14 012 (1998).

[5] S. Rakhmanova and D. L. Mills, Phys. Rev. B **54**, 9225 (1996).

[6] R. Lai and A. J. Sievers, Phys. Rev. B **57**, 3433 (1998); **55**, R11 937 (1997).

[7] A. M. Kosevich, B. A. Ivanov, and A. S. Kovalev, Phys. Rep. **194**, 117 (1990).

[8] R. Lai, S. A. Kiselev, and A. J. Sievers, Phys. Rev. B **54**, R12 665 (1996).